2015

Nonlinear response of lateral piles with compatible cap stiffness and p-multiplier

Wei Dong Guo
University of Wollongong, wdguo@uow.edu.au

Publication Details

Guo, W. (2015). Nonlinear response of lateral piles with compatible cap stiffness and p-multiplier. Journal of Engineering Mechanics, 141 (9), 06015002-1-06015002-11.

Nonlinear response of lateral piles with compatible cap stiffness and p-multiplier

Abstract
Response of lateral pile groups is modeled using the more accurate (than any other numerical modeling) p – y curves-based load transfer model. It is essentially underpinned by limiting force per unit length pmpu, modulus of subgrade reaction pmk, and p-multiplier pm (to cater for pile-pile interaction, pm ¼ 1 for single piles). With the model, new closed-form solutions are developed incorporating the cap-rotational stiffness kr. The solutions are presented in nondimensional charts for free-head (kr ¼ 0) through fixed-head (kr > 10 times the pile bending stiffness). The study reveals that the existing pm (bearing no link to the stiffness kr) is inconsistent with pm ¼ 0.25 for capped piles (at limiting state of elastic solutions). This casts doubt about the accuracy of available solutions, and a compatible stiffness kr and pm is required. The compatible normalized stiffness knr is equal to 0.275-0.333 (n ¼ 0.7) and 0.333-0.564 (n ¼ 1.7) for the associated pm at the design level of (ground-level) bending moment specified in the JGJ code. Use of the solutions is elaborated for a typical offshore pile group against measured response, which largely substantiates the deduced stiffness knr. The coupled kr and pm revealed are fundamental to design of the capped piles using any methods. The new solutions using the knr and pm values should be employed to conduct pertinent design.

Disciplines
Engineering | Science and Technology Studies

Publication Details
Guo, W. (2015). Nonlinear response of lateral piles with compatible cap stiffness and p-multiplier. Journal of Engineering Mechanics, 141 (9), 06015002-1-06015002-11.

Date revised: 10May, 2013; 21 Nov, 2014, March, 2015

Title: # Nonlinear response of lateral piles with compatible cap stiffness and *p*-multiplier

Wei Dong Guo, M. ASCE

Affiliation and address:
Associate Professor Wei Dong Guo
School of Civil, Mining & Environmental
Engineering
University of Wollongong, NSW 2522, Australia
Email: camsaweidguo@lycos.com; wdguo@uow.edu.au
Tel: (61-2) 4221 3036

Words: 5567
Number of tables: 1
Number of figures: 7

Key words: piles and pile groups, closed-form solutions, nonlinear response, lateral loading, soil-structure interaction

ABSTRACT

Response of lateral pile groups is modelled using the more accurate *p-y* curves based load transfer model (than any other numerical modelling). It is essentially underpinned by limiting force per unit length $p_m p_u$, modulus of subgrade reaction $p_m k$, and *p*-multiplier p_m (to cater for pile-pile interaction, p_m= 1 for single piles). With the model, new closed-form solutions are developed incorporating the cap-rotational stiffness k_r. The solutions are presented in non-dimensional charts for free-head (k_r = 0) through fixed-head (k_r > 10 times the pile bending stiffness*)*. The study reveals that

- The existing p_m (bearing no link to the stiffness k_r) is inconsistent with 'p_m= 0.25' for capped piles (at limiting state of elastic solutions). This casts doubt about the accuracy of available solutions; and a compatible stiffness k_r and p_m is required.
- The compatible normalised stiffness k_{nr} is equal to 0.275 ~0.333 (n = 0.7) and 0.333~0.564 (n = 1.7) for the associated p_m at the design level of (ground-level) bending moment specified in the JGJ code.

Use of the solutions is elaborated for a typical offshore pile group against measured response, which largely substantiates the deduced stiffness k_{nr}. The coupled k_r and p_m revealed are fundamental to design of the capped piles using any methods. The new solutions using the k_{nr} and p_m values should be employed to conduct pertinent design.

Key words: nonlinear response, rotating cap, limiting force profiles, lateral loading, piles

Introduction

Piles are customarily cast into a pile cap that restrains pile-head rotation (Mokwa and Duncan 2003; Ooi et al. 2004; Guo 2009), but allows horizontal translation during lateral loading. However at a working load level, cap-rotation generally occurs (Mokwa and Duncan 2003; Ooi et al. 2004), owing to relaxation of soil resistance underneath the pile-cap or around piles (Guo 2009), insufficent cap-restraint and possible cracking of the piles. The translation (displacement) and rotation [see Fig. 1(a)] may be associated with ~4 times different resistance as noted for rigid piles. This difference has to be properly considered to provide reliable design, especially, for wind-turbine foundations and subjected to earthquake loading.

Lateral pile-soil interaction may be mimicked using a series of independent springs-sliders distributed along the shaft and a membrane (to incorporate couple interaction among the springs) (e.g. Fig. 1(b)). The slider is characterised by the profile of limiting force per unit length (p_u profile) to a (slip) depth x_p, and the spring has a modulus of subgrade reaction k for the pile-soil system. In the context of the interaction model, elastic-plastic closed-form solutions (Guo 2012) were developed for free-head rotation but for soil resistance (FreH piles), and capped-head (no rotation, FixH piles), respectively. The FixH solutions are also used to predict group response using a reduced limiting resistance $p_m p_u$ and modulus $p_m k$ by incorporating the pile-pile interaction factor p_m (= p-multipliers ≤ 1.0) (Brown et al. 1998) [see Fig.1 (c) and (e)].

Fixed-head solutions using numerical finite element method, and finite difference approach (Ooi et al. 2004) overestimate measured maximum bending moment and underestimate measured deflection of capped piles (Duncan et al. 2005) at large; whereas free-head solutions offer incorrect depth of maximum bending moment and overestimate the head-deflection. The

concept of *p*-multiplier is less rigorous but offers more reliable and efficient prediction of overall pile response than finite element and finite difference methods (Guo 2009; Guo 2012). Nevertheless, the ~ 4 times difference in resistance due to cap-rotational stiffness $k_{r,}$ must be quantified to conform with the p_m to gain reliable solutions, which is not available. To meet more stringent design, new solutions underpinned by load transfer model are developed in this paper, for piles with a cap stiffness k_r. With the solutions, the impact of the stiffness k_r is examined and presented in non-dimensional charts. The stiffness k_r and the p_m are obtained for typical cases.

Overall Solutions for A Single Pile

Load Transfer Model

Fig. 1(b) shows under a pile-head load *H*, the pile-soil system is simulated using the uncoupled (with $N_p = 0$, plastic zone) and coupled ($N_p \neq 0$, elastic zone) load transfer models (Guo 2006). The pile-head has a rotational stiffness k_r, and a ground-level bending moment M_o of $k_r\omega_g$ (ω_g = pile-head rotation angle in radian, at zero loading eccentricity of $e_p = 0$). The pile-soil system retains the salient features of free-head ($k_r = 0$) and fixed-head piles ($k_r > 10E_pI_p$, E_pI_p = flexural stiffness of a pile), as recaptured in Appendix I. The net limiting force per unit length, p_u [FL^{-1}] along the pile shaft [see Fig. 1(c)] is the sum of the passive soil resistance acting on the face of the pile in the direction of soil movement, and sliding resistance on the side of the pile, less any force due to active earth pressure on the rear face of the pile. The p_u is described by (Guo 2006)

$$p_u = A_L (x + \alpha_o)^n \tag{1}$$

$$A_L = \tilde{s}_u N_g d^{1-n} \text{ (cohesive soil), and } A_L = \gamma_s' N_g d^{2-n} \text{ (cohesionless soil)} \tag{2}$$

where *d* is pile diameter [L]; *x* is depth below ground level [L]; α_o is an equivalent depth to include the p_u at ground-line level [L]; *n* is a power to the corrected depth of $x+ \alpha_o$; $\tilde{s}_u$ is an

average undrained shear strength s_u of the soil [FL^{-2}] over the max x_p anticipated; N_g is a gradient correlated clay strength or sand density to the limiting p_u; γ_s' is effective unit weight of the overburden soil [FL^{-3}] (i.e. dry weight above water table, and buoyant weight below). The parameters α_o, N_g, and n were deduced against measured response of 70 free-head piles and ~30 capped piles in single or layered soil (Guo 2013a). It is noted that n = 0.5~0.7 (for a uniform strength profile, e.g. clay), and 1.3~1.7 (for a linearly increasing strength profile. e.g. sand). The p_u along with a subgrade modulus k are sufficiently accurate to model pile response. The p_u [≤ 9.14~11.94$s_u d$ clay (Randolph and Houlsby 1984)] from equation (1) is only effective to the max x_p. It may be estimated using angle of internal friction and cohesion of a subsoil by Hansen's solution (Hansen 1961; Guo 2013a).

The uncoupled and coupled load transfer models (Hetenyi 1946; Guo and Lee 2001) allow the governing equations for the pile (see Fig. 1) to be obtained as

$$E_p I_p w^{IV}(x) = -p_u \qquad \text{(Elastic zone, } 0 \le x \le x_p\text{)} \qquad (3)$$

$$E_p I_p w^{IV}(z) - N_p w''(z) + kw(z) = 0 \qquad \text{(Plastic zone, } x_p \le x \le L\text{, or } 0 \le z \le L - x_p\text{)} \qquad (4)$$

where $w(x)$ is the pile deflection at depth x; $w^{IV}(x)$ is 4th derivative of $w(x)$ with respect to x; I_p and E_p are moment of inertia and Young's modulus of an equivalent solid cylindrical pile, respectively. As with those for free-head and fixed-head piles (Guo 2006), response of the lateral pile (see Fig. 1) is presented against the depth x (measured from ground level) in the upper plastic zone, and a depth z (= x- x_p, measured from the slip depth x_p) in the lower elastic zones, respectively, to generate compact expressions. The values of N_p and k are calculated using the average modulus G_s of the soil over the effective length L_c (see Appendix I).

Pile-head Rotational Stiffness k_r

A laterally loaded pile group generally exhibts the cap-rotation owing to more compression in piles located in front rows than back rows. The rotational stiffness of the pile-cap k_r may be taken as that of pile-head for a fully cast concrete cap with a sufficient rigidity. It may then be calculated using axial stiffness and capacity of a single pile, with due account of the pile group spacing (Mokwa and Duncan 2003). This treatment, however, is not valid to capped single piles or pile groups with other head constraints. The rotational stiffness k_r does affect the magnitude of the p_u (Guo 2009), which may be determined using N_g [see Eq. (2)]. A fictitious gradient N_g^{FreH*} is deduced by matching a measured load-displacement relationship (indicated by an asterisk * in the N_g) with free-head solutions; and a N_g^{FixH*} with fixed-head solutions. Elastic theory for a laterally loaded rigid pile (Scott 1981; Guo 2012) provides $w_g^{FixH} = H^{FixH}/k^{FixH}L$, and $w_g^{FreH} = 4H^{FreH}/k^{FreH}L$. Assuming that $4w_g^{FixH} = w_g^{FreH}$ and $p_m k^{FreH} = k^{FixH}$ leads to $p_m H^{FixH} = H^{FreH}$, which renders at limit state $p_m N_g^{FixH*} = N_g^{FreH*}$. This, by no means, indicates a factor of p_m between fixed-head and free-head N_g, as the 4 times different displacements would not be warranted between the piles. In fact the ratio becomes far greater than 4 once plastic deformation is induced (Guo 2013b). The form of $N_g^{FixH*} = p_m N_g^{FreH}$ is adopted here to deduce N_g with a stiffness k_r.

Ground-level bending moment M_o may be measured for a lateral load H at a loading eccentricity e_p above ground level. Owing to semi-fixity, the Chinese JGJ design code (JGJ 1994) recommends a design bending moment M_o be 0.4 times the moment (denoted as M_o^{FixH}) induced on a pile-head with translation only (FixH) pile; and the design pile-head deflection w_g be 1.25 times the w_g^{FixH} gained using the FixH solutions (JGJ 1994). The ratios will be used later to determine the stiffness k_r.

Elastic-plastic Solutions

Equations (3) and (4) were resolved using the technology for free-head piles (Guo 2006) by enforcing the bending moment $-M_o = E_p I_p w''(0) = k_r \omega_g + He_p$, and the shear force $-Q(0) = H$ at the pile-head level ($x = 0$). Note the ω_g is of a negative value, and offers a counter moment against He_p as expected. The elastic-plastic solutions developed are provided in Appendix I for response profiles and head response, respectively. They involve the reciprocal of a characteristic length λ [$= \sqrt[4]{k/(4E_p I_p)}$], the on-pile force per unit length $p = p_u$ at $x \le x_p$ [see Fig. 1(c)], the normalised ground-level resistance $\overline{\alpha}_o$ ($= \lambda\alpha_o$), and the two coupled parameters α_N and β_N in elastic zone ($\alpha_N = \beta_N = 1$ for uncoupled springs with $N_p = 0$). The response profiles are dominated by the normalised depths $\bar{x}$ ($= \lambda x$) and $\bar{z}$ ($= \bar{x} - \bar{x}_p$, $\bar{x}_p = \lambda x_p$), respectively for plastic and elastic zones, and involve normalised pile-head load $\overline{H}$ ($= H\lambda^{n+1}/A_L$), ground-level deflection w_g (via $\overline{w}_g = w_g k\lambda^n/A_L$) and rotation ω_g (via $\overline{\omega}_g = \omega_g k\lambda^{n-1}/A_L$) for the normalised stiffness k_{nr} [$= k_r\lambda^3/k$].

Simplified Expressions

The dimensionless expressions of $\overline{H}$, $\overline{w}_g$, and $\overline{\omega}_g$ (see Appendix I) largely reflect the consequence of mobilization depth (via $\bar{x}_p$) of the limiting force per unit length p_u along a laterally loaded pile. They may be simplified to the following form, given negligible on-pile resistance at ground-line and the coupled interaction (thus $\alpha_o \approx 0$ and $N_p \approx 0$).

$$\overline{\omega}_g = \frac{\bar{x}_p^n}{2(\bar{x}_p+1)^2 k_{nr} + 1 + \bar{x}_p + \bar{e}_p} \left\{ \begin{array}{l} \dfrac{4\bar{x}_p^3(\bar{x}_p + \bar{e}_p + 1)}{(n+1)(n+2)(n+3)} + 2\bar{x}_p^2 \dfrac{(1 - \bar{x}_p^2 - 2\bar{x}_p\bar{e}_p)}{(n+1)(n+2)} \\ -2\bar{x}_p \dfrac{\bar{x}_p(1+\bar{x}_p) + (1+2\bar{x}_p)\bar{e}_p}{n+1} - (1+\bar{x}_p)(1+\bar{x}_p+2\bar{e}_p) \end{array} \right\} \quad (5)$$

$$\overline{H} = \frac{0.5\bar{x}_p^n[(n+1)(n+2)+2\bar{x}_p(2+n+\bar{x}_p)]}{(\bar{x}_p+1+\bar{e}_p)(n+1)(n+2)} - \frac{k_{nr}\overline{\omega}_g}{\bar{x}_p+1+\bar{e}_p} \quad (6)$$

$$\overline{w}_g = -\overline{\omega}_g\bar{x}_p\left(\frac{2k_{nr}\bar{x}_p(2\bar{x}_p+3)}{3(\bar{x}_p+\bar{e}_p+1)}+1\right) + \frac{4\bar{x}_p^{4+n}}{(n+1)(n+2)(n+3)(n+4)} - \frac{\left[2\bar{x}_p^2+(2\bar{x}_p+n+1)(n+2)\right](\bar{x}_p+3\bar{e}_p)\bar{x}_p^{2+n}}{3(1+\bar{x}_p+\bar{e}_p)(n+1)(n+2)} + \bar{x}_p^n \quad (7)$$

where $k_{nr} = k_r\lambda^3/k = 4k_r/(E_pI_p\lambda) = \bar{k}_r/\overline{\omega}_g$. The maximum bending moment is likely equal to the ground-line moment M_o (with $\overline{M}_o = \overline{H}\bar{e}_p + k_{nr}\overline{\omega}_g$) for semi-FixH piles. The solutions possess similar features to FreH and FixH solutions (Guo and Lee 2001; Guo 2006) (see Appendix I), but for the N_g and n (thus A_L) values. The impact of the stiffness k_r is significant, but there is no simple way to estimate its value. The k_r may be calculated from the upper structure behaviour as suggested in some numerical program manuals, but this is often hard to be achieved. Assuming a design ratio M_o/M_o^{FixH}= 0.4 (JGJ 1994), the k_r is deduced here using Eqs. (5) and (6) for elastic case, which is simplified as Eq. (8) for e_p = 0.

$$\frac{\overline{\omega}_g k_{nr}}{\overline{\omega}_g k_{nr}^{FixH}} = \frac{\omega_g k_{nr}}{\omega_g k_{nr}^{FixH}} p_m^{0.25(n-1)} = \frac{M_o}{M_o^{FixH}} p_m^{0.25(n-1)} \quad (8)$$

The FixH condition is enforced using a k_{nr}^{FixH} (ie. k_{nr} for fully fixed-head) = 50,000, although 'k_{nr} > 50' is sufficiently accurate. The k_{nr} values are determined for n = 0.7 and 1.7, which describe most piles well in clay and sand, respectively. Using Eq. (8) (taking $\bar{x}_p$ = 0.0001) and M_o/M_o^{FixH} = 0.4, the k_{nr} at n = 0.7 was deduced as 0.275 ~ 0.333 with k_{nr}/p_m = 0.275/0.2, 0.288/0.3, 0.298/0.4, 0.306/0.5, 0.313/0.6, 0.319/0.7, 0.324/0.8, 0.329/0.9, and 0.333/1.0, respectively; and k_{nr}(at n = 1.7) = 0.333~0.564, or more specifically k_{nr}/p_m = 0.564/0.2, 0.488/0.3, 0.443/0.4, 0.412/0.5, 0.389/0.6, 0.371/0.7, 0.356/0.8, 0.344/0.9, and 0.333/1.0, respectively. These values

may be used in initial design in light of the JGJ code. Note a k_{nr} = 0.5 for n = 0.7~1.7 is deduced using Eq. (9) for elastic case, and w_g/w_g^{FixH} = 1.25 (JGJ 1994), which is yet to be confirmed.

$$\frac{\overline{w}_g}{\overline{w}_g^{FixH}} = \frac{w_g}{w_g^{FixH}} p_m^{0.25n} \tag{9}$$

Validation and Parametric Analysis

The newly established closed-form (CF) solutions reduce to those for free-head piles at k_{nr} = 0 (Guo 2006) and for fixed-head piles at k_{nr} > 50 (Guo 2009), which compare well with finite element approach and experimental data. Thereby, the nonlinear response of capped piles was examined for a rotational stiffness $k_r = (0\sim10)E_pI_p\lambda$ at the typical n = 0.7 and 1.7, respectively. Given n = 0.7, normalised load ($\overline{H}$)-displacement ($\overline{w}_g$) curves at ground level are depicted in Fig. 2(a), and displacement ($\overline{w}_g$) - bending moment ($\overline{M}_o$) curves in Fig. 2(b), respectively. The same response concerning n = 1.7 is plotted in Fig. 3(a) and (b). The normalised displacement ($\overline{w}_g$) versus rotational ($\overline{\omega}_g$) response is presented in Fig. 4(a) and (b) for n = 0.7 and 1.7, respectively. The profiles of non-dimensional displacement, slope, bending moment and shear force, for example at $\bar{x}_p$ = 1 are illustrated in Fig. 5(a) through (d) for n = 0.7; and in Fig. 6(a) through (d) concerning n = 1.7. The impact of the rotational stiffness on the response is evident in Figs. 2 through 6. This is elaborated next in an example.

A Pile in 10-pile Group in Clay (Matlock et al. 1980)

Matlock et al (1980) performed lateral loading tests on a single pile, two circular groups with 5-pile and 10-pile, respectively in Harvey, Louisiana. The tests were conducted in a pit 2.4 m deep.

The site consists of a highly plastic gray-clay with an occasional thin layer of peat, sand or silt within a depth of 2.4 m - 18 m. The plasticity index was 77~100 (at a depth 0~1.2 m below the test pit) and 100~185 (1.2~2 m below), respectively, which allow the angle of the soil friction ϕ (drained case) to be estimated as 12 degree (BSI 1985), and a cohesion c as 1 kPa (Guo 2013a).

The 10-pile group is analysed herein. The tubular steel piles were installed in a circle [see Fig. 7(a)] at a center-to-center spacing of 1.8 pile diameters. Each was 13.4 m in length, 168 mm in outside diameter, 7.1 mm in wall thickness, and had a bending stiffness of 2.326 MN-m^2. The piles were driven 11.6 m into a uniform soft clay that had a undrained shear strength s_u of 20 kPa. Deflections of the group during the tests were enforced at two support levels (of 0.305 and 1.83 m) above ground-line to mimic FixH restraints. The measured H_{av}-w_t and w_t-M_o curves for a pile in the group are plotted in Fig. 7(c) and (d), respectively. The measured bending moment profiles are plotted in Fig. 7(e) for four typical values of ground-level deflection w_g.

The response of a capped pile in the group was predicted using free-head and fixed-head solutions (Guo 2012), n = 0.85, p_m = 0.2 (for either solution), $G_s = 13s_u$ (fixed-head solutions) or $33s_u$ (free-head solutions), and the respective, fictitious profile of limiting force per unit length p_u [Fig. 7(b)]. Note the correlation of $G_s^{FixH} \approx 0.39G_s^{FreH}$ is resulted from semi-fixed head constraints and less interaction from the special (circle) layout of the group, otherwise $G_s^{FixH} = p_m G_s^{FreH}$. The curves of average load per pile (H_{av}) versus mudline deflection (w_g) predicted are plotted in Fig. 7(c), which agree remarkably well with the measured H_{av}-w_t curve (thus $w_t \approx w_g$). The predicted M_o values using fixed-head solutions are much higher than the measured values [see Fig. 7(d) and 7(e)] (Guo 2009), even after deducting the moment $H_{av}e_p$ caused by loading eccentricity above ground level e_p). The new solutions are next used to examine impact of rotational stiffness k_r on the modulus G_s, the limiting force per unit length p_u, and the response of

a pile in the group. It is based on revised modulus G_s and p_u using a partial factor α_r (rather than the p_m) determined iteratively. The α_r is initially taken as the ratio of M_o/M_o^{FixH} (JGJ 1994).

First, assuming a factor α_r = 0.42, the modulus G_s was taken as $G_s^{FixH*} + \alpha_r(G_s^{FreH*} - G_s^{FixH*})$. Given $G_s^{FixH*} = 13s_u$, $G_s^{FreH*} = 33s_u$, the G_s is estimated as $25s_u$ [= $13s_u + \underline{0.42}\times(33\text{-}13)s_u$, or $p_m = 0.76 = G_s/G_s^{FreH*}$]. This yields k= 1.59×10^3 kPa (= 3.18G_s, s_u= 20 kPa), and λ = 0.643/m {= $[k/(4\times2.326)]^{0.25}$}.

Second, the maximum p_u profile was estimated using Hansen's expression for free-head piles with c = 1 kPa, and ϕ = 12^o, and is plotted in Fig. 7(b). As with the calculation of $\boldsymbol{G_s}$, the A_L is estimated as $2.26A_L^{FixH*}$ using $A_L^{FixH*} + \alpha_r(A_L^{FreH*} - A_L^{FixH*})$, and A_L^{FreH*}= $4A_L^{FixH*}$, or p_m = 0.565 = A_L/A_L^{FreH*}. Note this p_m value should be the same as that for calculating the shear modulus, but for the special group layout (Guo 2009). The A_L is calculated as 5.22 kN/m$^{1.85}$ (= 1×20×0.1681$^{-0.15}$×0.2) (Guo 2009), which was reduced to 5.142 kN/m$^{1.85}$ to compensate the impact from using e_p = 0 against a real e_p (> 0). With n = 0.85, and A_L = 5.142 kN/m$^{1.85}$, the p_u profile was obtained and is plotted in Fig. 7(b) as Guo LFP. It matches well with the Hansen LFP. Both Guo LFP and Hansen LFP offer weaker or slightly stronger (above or below a depth of 15d) resistance than the Bogard & Matlock's p_u does. This difference has limited impact on the pile response (with a maximum x_p of 22.14d).

Third, with A_L, n, and k, the λ is calculated, normalised load $\overline{H}$, moment (thus $\overline{\omega}_g$ with a known $\overline{e}_p$), and displacement $\overline{w}_g$ are obtained for measured load H, ground-level bending moment M_o at a typical displacement w_g. The three measured values allow the three unknown k_{nr}, A_L (thus α_r) and $\overline{x}_p$ (via k) to be resolved iteratively using Eqs. (5), (6) and (7). The α_r value should be within an acceptable difference to the assumed value, otherwise, a new α_r is

stipualated (resulting in new G_s, A_L, and k), the three steps are repeated. The calculation can be readily done using a professional mathmatical program (e.g. Mathcad^{TM}).

This iterative calculation is illustrated using the design chart for n = 0.7 (note n = 0.85 for the current pile), which encompasses three steps: (1) a pair of measured load H and displacement w_g are normalised, respectively, using A_L, n, and k gained for free-head piles (e.g. $\overline{H}$ = 1.56 at $\overline{w}_g$ = 10, see bold values in Table 1). (2) The pair $\overline{H}$ and $\overline{w}_g$ allow $k_r/(E_pI_p\lambda)$ = 1.1 (or k_{nr} = 0.275) to be ascertained in Fig. 2(a), which gives a stiffness k_r of 1.643 MNm (= $1.1E_pI_p\lambda$). (3) The α_r is estimated using $\overline{H}$ (measured) = $\overline{H}^{\text{FixH*}} + \alpha_r(\overline{H}^{\text{FreH*}} - \overline{H}^{\text{FixH*}})$. For instance, at $\overline{w}_g$ = 10, $\overline{H}^{\text{FixH*}}$ = 1.0 and $\overline{H}^{\text{FreH*}}$ = 2.2 [see Fig. 2(a)], and $\overline{H}$ (measured) = 1.5, the α_r is obtained as 0.42 from 1.5 = 1.0 + α_r(2.2-1). The deduced values are k_{nr} = 0.275 and α_r = 0.42 for the measured $\overline{H}$ and $\overline{w}_g$. The calculation may be repeated for other measured pairs of $\overline{H}$ and $\overline{w}_g$, and similar k_{nr} and α_r should be obtained (Guo 2013a).

With the p_u (n = 0.85), the G_s and the k_{nr} (= 0.275) obtained, the pile response is readily predicted. This is provided next for e_p = 0 (zero loading eccentricity) for a ground-level deflection w_g of 9.4, 23.5, 47.3 and 83.1 mm (at which bending moment profiles are provided). With w_g = 9.4 mm, normalised slip depth $\overline{x}_p$ is estimated as 0.863 (x_p = 1.342 m). (1) The $\omega_g k\lambda^{n-1}/A_L$ is calculated using Eq. (5).

$$\frac{\omega_g k\lambda^{-0.15}}{A_L} = \frac{-0.863^{0.85}}{1.863\times 2\times 0.275+1}\left(\frac{2\times 0.863^2[0.863+3+0.85]}{2.85\times 3.85}+1+0.863\right) = -1.091 \qquad (10)$$

Likewise, the values of $H\lambda^{1.85}/A_L$ = 0.686 and $w_g k\lambda^{0.85}/A_L$ =1.997 were obtained using Eqs. (6) and (7), respectively, along with $-M_o\lambda^{2.85}/A_L$ = 5.427. (2) With k = 1.59×10^3 kPa and A_L= 5.142 kN/m$^{1.85}$, the ground-level rotation angle ω_g = - 3.3035×10^{-3}, and H = 7.981 kN were obtained at

w_g= 9.4 mm. (3) With expressions in Appendix I, $F(1,0)= F(2,0)= 0$, constants C_5= 4.154×10^{-3} and C_6= -1.574×10^{-3} were obtained respectively. The pile deflection at depth x (plastic zone) or z (elastic zone) is calculated respectively as

$$w(x)=\frac{5.142}{E_pI_p}\left[\frac{-x^{4.85}}{4.85\times3.85\times2.85\times1.85}+\frac{1.33017x^3-2.7135x^2}{5.142}-(3.3035x-9.4)\times10^{-3}\right]\ \text{(m)} \quad (11a)$$

$$w(z)=e^{-0.643(x-1.342)}\{4.154\cos[0.643(x-1.342)]-1.574\sin[0.643(x-1.342)]\}\times10^{-3}\ \text{(m)} \quad (11b)$$

The profile of bending moment $M(\bar{x})$ or $M(\bar{z})$ is obtained as

$$\begin{aligned}-M(x)&=-\frac{x^{2+n}A_L}{(n+2)(n+1)}+Hx+k_r\omega_g\\&=-\frac{5.142\,x^{2.85}}{1.85\times2.85}+7.98x+1.645\times10^3\times(-3.3035\times10^{-3})\end{aligned} \quad (12a)$$

$$\begin{aligned}-M(\bar{z})&=2E_pI_p\lambda^2e^{-\bar{z}}[-C_6\cos(\bar{z})+C_5\sin(\bar{z})]\\&=1.923\times10^3e^{-0.643(x-x_p)}\{-C_6\cos[0.643(x-x_p)]+C_5\sin[0.643(x-x_p)]\}\end{aligned} \quad (12b)$$

The calculated bending moment profile is plotted in Fig. 7(e) as a solid line.

As with w_g = 9.4 mm, the normalised slip depth $\bar{x}_p$ was estimated as 1.3484, 1.7823, and 2.1764 for w_g= 23.5, 47.3 and 83.1 mm respectively. The H, ω_g, C_5 and C_6 values (see Table 1) were obtained; and the bending moment profiles are plotted in Fig. 7(e). The predicted moment profiles agree well with the respective measured data but not the fixed–head predictions (via the program GASLGROUP). Note the profile of shear force $Q(\bar{x})$ or $Q(\bar{z})$ (not shown herein) can be predicted using the expressions in Appendix I.

Importantly, this capped pile has a moment ratio M_o/M_o^{FixH} of 0.371~0.442 (with 0.442, 0.396, 0.377 and 0.371 at w_g = 9.4, 23.5, 47.3, and 83.1 mm, respectively, see Table 1). The average (of 0.406) is rather close to 0.4 specified by the JGJ code, despite the special group layout, cap configuration, and nonlinear response. This consistency is further echoed between

the deduced values of k_{nr}/p_m = 0.275/0.565 ~ 0.76 (for M_o/M_o^{FixH} = 0.371~0.442) and the theoretical values of 0.31/0.565 (for M_o/M_o^{FixH} = 0.4). The reliability of the current solutions and the k_{nr} and p_m values is thus vindicated.

Conclusions

Response of lateral pile groups is modelled using the more accurate *p-y* curves based load transfer model (than any other numerical modelling). It is essentially underpinned by limiting force per unit length $p_m p_u$, modulus of subgrade reaction $p_m k$, and *p*-multiplier p_m (to cater for pile-pile interaction, p_m= 1 for single piles). With the model, new closed-form solutions are developed incorporating the cap-rotational stiffness k_r. The solutions are presented in non-dimensional charts for free-head (k_r = 0) through fixed-head ($k_r > 10E_pI_p$). The study reveals that

- The existing p_m (bearing no link to the stiffness k_r) is inconsistent with 'p_m= 0.25' for capped piles (at limiting state of elastic solutions). This casts doubt about the accuracy of available solutions; and a compatible stiffness k_r and p_m is required.
- The compatible normalised stiffness k_{nr} is equal to 0.275 ~0.333 (n = 0.7) and 0.333~0.564 (n = 1.7) for the associated p_m at the design level of (ground-level) bending moment specified in the JGJ code.

Use of the solutions is elaborated for a typical offshore pile group against measured response, which largely substantiates the deduced stiffness k_{nr}. The coupled k_r and p_m revealed are fundamental to design of the capped piles using any methods. The new solutions using the k_r and p_m values should be employed to conduct pertinent design.

NOTATION

The following symbols are used in the paper:

294 A_L = coefficient for the LFP;

295 c = cohesion;

296 d = diameter of an equivalent solid cylinder pile;

297 E_p = Young's modulus of an equivalent solid cylinder pile;

298 e, e_p, = eccentricity (= e_p), eccentricity of the location above the ground level for applying the
299 $H(H_g)$;

300 E_pI_p = flexural stiffness of a lateral pile;

301 *FreH* = free head, allowing translation and rotation at head-level;

302 *FixH* = fixed-head, allowing translation but not rotation at head level;

303 G_s , G^* = average soil shear modulus over the critical length, L_c, and $G^* = (1+0.75\nu_s)G_s$;

304 I_p = moment of inertia of an equivalent solid cylinder pile;

305 k = modulus of subgrade reaction;

306 $K_i(\gamma)$ = modified Bessel function of second kind of i^{th} order (Appendix I);

307 L, L_c = embedded pile length, and critical length beyond which any increase in the embedment
308 would not affect the pile response;

309 LFP = the profile of net limiting force per unit pile length;

310 M_o, $M(\bar{x})$ = bending moment at the mudline level; the moment at the normalised depth $\bar{x}$;

311 $\overline{M}_o$ = $M_o\lambda^{2+n}/A_L$, normalised M_o;

312 n, = power for the LFP;

313 N_g, = gradient correlated soil strength to the p_u, deduced from measured load-displacement of
314 a capped pile using current solutions;

315 N_g^{FreH}, N_g^{FixH} = gradient N_g deduced from measured load-displacement using the free- and fixed-
316 head piles, respectively;

317 N_p = fictitious tension for the membrane tied together the springs around the pile shaft;

318 H = lateral load exerted on a single pile;

319 $\overline{H}$ = $H\lambda^{1+n}/A_L$, normalised pile-head load;

320 H_{av}, H_g= average load per pile in a group, and total load imposed on a group;

321 k_{nr} = $k_r\lambda^3/k = 4k_r/(E_pI_p\lambda) = \bar{k}_r/\bar{\omega}_g$, and $\bar{k}_r = k_r\omega_g\lambda^{2+n}/A_L$;

322 k_r = rotational stiffness of the pile cap;

323 p_m = p-multipliers used to reduce stiffness, and limiting force for individual piles in a group;

324 p_u = limiting force per unit length;

325 $p(\bar{x})$,$Q(\bar{x})$ = net force per unit length, and shear force at the normalised depth $\bar{x}$;

326 $s_u(\tilde{s}_u)$ = undrained shear strength of soil (Average s_u over a maximum slip depth anticipated);

327 t = wall thickness of a pipe pile;

328 x, x_p, $\bar{x}$, $\bar{x}_p$ = depth below ground level, slip depth from elastic to plastic state, $\bar{x} = \lambda x$, $\bar{x}_p = \lambda x_p$;

329 w, $w(x)$, $w(z)$ = lateral deflection of a pile, w in the plastic, and w in elastic zone, respectively;

330 $\bar{w}_g$ = $w_g k\lambda^n/A_L$ normalised mudline deflection;

331 w_p = local limiting deflection beyond which the force mobilised on the depth is p_u;

332 w_t, w_g = pile deflection at loading level, and the deflection at mudline;

333 $w(\bar{x})$, $w'(\bar{x})$ = deflection and rotation at the normalised depth $\bar{x}$;

334 z, $\bar{z}$ = depth below the slip depth x_p (i.e. $z = x - x_p$), and $\bar{z} = \lambda z$, respectively;

335 α_N, β_N = normalised stiffness factors;

336 $\alpha_o(\bar{\alpha}_o)$ = an equivalent depth to account for ground level limiting force with $\bar{\alpha}_o = \alpha_o\lambda$;

337 α_r = a partial factor to gain the A_L and G_s using those for free-head and fixed-head piles;

338 γ = load transfer factor (Appendix I);

339 γ_s' = effective unit weight of the overburden soil;

340 ϕ = angle of internal friction of soil;

341 ω_g = rotation angle of pile at ground-level

342 $\bar{\omega}_g$ = $\omega_g k\lambda^{n-1}/A_L$, normalised mudline rotation;

343 λ = reciprocal of characteristic length;

344 ν_s = Poisson's ratio of soil, taken as 0.25 for sand, otherwise 0.4;

345 Superscript '*'denotes parameters deduced by matching the same pile response using free-head
346 and fixed-head solutions; Subscript 'g' for ground level; 's' soil.

347

348

References

Brown, D. A., C. Morrison and L. C. Reese (1998). "Lateral load behaviour of pile group in sand." Journal of Geotechnical and Geoenvironmental Engineering Division, ASCE, Vol. 114**,** No.11: pp.1261-1276.

BSI (1985). Structural use of concrete. BS 8110, London, Parts 1–3.

Duncan, J. M., M. D. Robinette and R. L. Mokwa (2005). Analysis of laterally loaded pile groups with partial pile head fixity. Advances in Deep Foundations, GAS 132, ASCE.

Guo, W. D. (2006). "On limiting force profile, slip depth and lateral pile response." Computers and Geotechnics, Vol. 33**,** No.1: pp.47-67.

Guo, W. D. (2009). "Non-linear response of laterally loaded piles and pile groups." International Journal for Numerical and Analytical Methods in Geomechanics, Vol. 33**,** No.7: pp.879-914.

Guo, W. D. (2012). Theory and practice of pile foundations. Boca Raton, London, New York, CRC press, Taylor & Francis Group.

Guo, W. D. (2013a). "Simple model for nonlinear resposne of 52 laterally loaded piles." Journal of Geotechnical and Geoenvironmental Engineering Division, ASCE, Vol. 139**,** No.2: pp.234-252.

Guo, W. D. (2013b). "Laterally loaded rigid piles with rotational constraints." Computers and Geotechnics, Vol. 54**,** No.2: pp.72-83.

Guo, W. D. and F. H. Lee (2001). "Load transfer approach for laterally loaded piles." International Journal for Numerical and Analytical Methods in Geomechanics, Vol. 25**,** No.11: pp.1101-1129.

Hansen, B. J. (1961). The ultimate resistance of rigid piles against transveral forces. Copenhagen, Denmark, The Danish Geotechnical Institute Bulletin No. 12.

Hetenyi, M. (1946). Beams on elastic foundations. Ann Arbor, University of Michigan Press.

JGJ (1994). (Chinese) Technical code for building pile foundations. JGJ 94-94, Beijing: 252.

Matlock, H., B. Wayne, A. E. Kelly and D. Board (1980). Field tests of the lateral load behaviour of pile groups in soft clay. Paper No. OTC. 3871, Proceedings of 12th annual offshore technology conference, Houston, Texas, 671-686.

Mokwa, R. L. and J. M. Duncan (2003). "Rotational restraint of pile caps during lateral loading." Journal of Geotechnical and Geoenvironmental Engineering Division, ASCE, Vol. 129**,** No.9: pp.829-837.

Ooi, P. S. K., B. K. F. Chang and S. Wang (2004). "Simplified lateral load analyses of fixed-head piles and pile groups." Journal of Geotechnical and Geoenvironmental Engineering Division, ASCE, Vol. 130**,** No.11: pp.1140-1151.

Randolph, M. F. and G. T. Houlsby (1984). "The limiting pressure on a circular pile loaded laterally in cohesive soil." Geotechnique, Vol. 34**,** No.4: pp.613-623.

Scott, R. F. (1981). Foundation analysis. N. J., Prentice Hall, Englewood Cliffs.

APPENDIX I – Solutions for Semi-fixed head piles

This appendix provides load transfer approach and solutions for semi-fixed head piles.

Assumptions and features of load transfer approach

- The springs are characterized by an idealised elastic-plastic *p*-*y* (*w*) curve [see Fig. 1(e)], which constitute, respectively, the uncoupled (N_p = 0) and coupled load transfer models for the plastic and elastic zones that transfer at a 'slip' depth x_p.
- The *k* and N_p for elastic zone are gained theoretically as (Guo and Lee 2001):

$$k = \frac{3\pi G_s}{2}\left\{2\gamma\frac{K_1(\gamma)}{K_0(\gamma)} - \gamma^2\left[\left(\frac{K_1(\gamma)}{K_0(\gamma)}\right)^2 - 1\right]\right\} \text{ and } N_p = \pi r_o^2 G_s\{[K_1(\gamma)/K_0(\gamma)]^2 - 1\}$$

where $K_i(\gamma)$ is modified Bessel function of second kind of i^{th} order (i = 0, 1); $\gamma = 0.65(E_p/G^*)^{-0.5}(L/r_o)^{-0.04}$(for long fixed-head piles with $L > L_c$ + max. x_p); G^* = $(1+3\nu_s/4)G_s$; r_o = 0.5d, radius; G_s is an average over a depth of L_c + max. x_p; and L_c = $1.05d(E_p/G_s)^{0.25}$. The expression for k_r = 0 (Guo 2013a) may be used to gain the modulus ratio of k/G_s for caps with rotational stiffness using an equivalent loading eccentricity e (= $e_p+k_r\omega_g/H$, ω_g/H is calculated for an average load level H and using k for e = 0).

- At the slip depth, x_p, the pile deflection $w(x_p)$ equals the limiting w_p (= p_u/k, and $p = p_u$ with $x < x_p$, see Fig. 1(d)). Below the x_p ($x \geq x_p$), the deflection $w(x)$ is less than w_p; and the resistance p (= $kw(x) < p_u$ at the depth) is linearly proportional to the k. The p_u profile (or LFP) is described by the parameters N_g, α_o, and n gained using average soil properties over a maximum slip depth x_p.
- In plastic zone, interaction among the springs is negligible (i.e. N_p = 0, Figure 1), as it cannot be transferred in the plastic zone. The resistance per unit length, p is fully mobilised to p_u. The N_p (in vertical direction), regardless of its value, does not involve in the governing equation for plastic zone.
- Pile-soil relative slip [e.g. value of $w(x)$-w_p] can only be initiated from mudline, and it can only move downwards.

Response profiles of a semi fixed-head pile

Response profiles in plastic zone **(** $\bar{x} \le \bar{x}_p$ **)** are given by

$$w(\bar{x}) = \frac{4A_L}{k\lambda^n}\{-F(4,\bar{x}) + F(4,0) + F(3,0)\bar{x} + [k_{nr}\bar{\omega}_g + \bar{H}\bar{e}_p + F(2,0)]\frac{\bar{x}^2}{2} + [F(1,0) + \bar{H}]\frac{\bar{x}^3}{6}\} + \frac{\omega_g}{\lambda}\bar{x} + w_g$$

$$w'(\bar{x}) = \frac{4A_L\lambda}{k\lambda^n}\left[-F(3,\bar{x}) + F(3,0) + [k_{nr}\bar{\omega}_g + \bar{H}\bar{e}_p + F(2,0)]\bar{x} + [F(1,0) + \bar{H}]\frac{\bar{x}^2}{2}\right] + \omega_g$$

$$-M(\bar{x}) = E_p I_p w''(x) = \frac{A_L}{\lambda^{2+n}}[-F(2,\bar{x}) + F(2,0) + (F(1,0) + \bar{H})\bar{x} + k_{nr}\bar{\omega}_g + \bar{H}\bar{e}_p]$$

$$-Q(\bar{x}) = E_p I_p w'''(x) = \frac{A_L}{\lambda^{1+n}}\left[-F(1,\bar{x}) + F(1,0) + \bar{H}\right]$$

where $\bar{k}_r = k_r\omega_g\lambda^{2+n}/A_L = k_{nr}\bar{\omega}_g$; $F(m,\bar{x}) = (\bar{x} + \bar{\alpha}_o)^{n+m}/(n+m)...(n+2)(n+1)$ $(1 \le m \le 4)$; $\bar{\alpha}_o = \lambda\alpha_o$; $F(0,\bar{x}) = (\bar{x} + \bar{\alpha}_o)^n$; and $\bar{e}_p = \lambda e_p$. Note both ω_g and $\bar{\omega}_g$ are used in the $w(\bar{x})$ expression.

Response profiles in elastic zone ($\bar{x} > \bar{x}_p$, or $\bar{z} > 0$, $\bar{z} = \lambda z = \lambda(x - x_p)$) are as follows:

$$w(\bar{z}) = e^{-\alpha_N\bar{z}}[C_5\cos(\beta_N\bar{z}) + C_6\sin(\beta_N\bar{z})]$$

$$w'(\bar{z}) = \lambda e^{-\alpha_N\bar{z}}[(-\alpha_N C_5 + \beta_N C_6)\cos(\beta_N\bar{z}) + (-\beta_N C_5 - \alpha_N C_6)\sin(\beta_N\bar{z})]$$

$$\begin{aligned}-M(\bar{z}) &= E_p I_p w''(z)\\ &= E_p I_p\lambda^2 e^{-\alpha_N\bar{z}}\{[(\alpha_N^2 - \beta_N^2)C_5 - 2\alpha_N\beta_N C_6]\cos(\beta_N\bar{z}) + [2\alpha_N\beta_N C_5 + (\alpha_N^2 - \beta_N^2)C_6]\sin(\beta_N\bar{z})\}\end{aligned}$$

$$\begin{aligned}-Q(\bar{z}) = E_p I_p w'''(z) = E_p I_p\lambda^3 e^{-\alpha_N\bar{z}}\{&[-\alpha_N(\alpha_N^2 - 3\beta_N^2)C_5 + \beta_N(3\alpha_N^2 - \beta_N^2)C_6]\cos(\beta_N\bar{z})\\ &+ [-(3\alpha_N^2 - \beta_N^2)\beta_N C_5 - \alpha_N(\alpha_N^2 - 3\beta_N^2)C_6]\sin(\beta_N\bar{z})\}\end{aligned}$$

where

$$C_5 = \frac{2A_L}{k\lambda^n}\{(1-2\alpha_N^2)[F(2,\bar{x}_p) - F(2,0) - k_{nr}\bar{\omega}_g - \bar{H}\bar{e}_p] - \alpha_N F(1,\bar{x}_p) + [\alpha_N - (1-2\alpha_N^2)\bar{x}_p][F(1,0) + \bar{H}]\}$$

$$C_6 = \frac{2A_L}{k\beta_N\lambda^n}\{\alpha_N(2\alpha_N^2 - 3)\{-F(2,\bar{x}_p) + F(2,0) + [F(1,0) + \bar{H}]\bar{x}_p + k_{nr}\bar{\omega}_g + \bar{H}\bar{e}_p\} + (\alpha_N^2 - 1)[-F(1,\bar{x}_p) + F(1,0) + \bar{H}]\}$$

$$\alpha_N = \sqrt{1 + N_p/\sqrt{4E_p I_p k}}, \quad \beta_N = \sqrt{1 - N_p/\sqrt{4E_p I_p k}}$$

These expressions are independent of the head constraint, and are identical to those for free-head piles.

$\bar{H}$, $\bar{w}_g$ and $\bar{M}_o$ of a semi fixed-head pile

(a) Normalised pile-head load, $\bar{H}$

439 $$\overline{H} = \frac{F(2,\bar{x}_p) - F(2,0) + \alpha_N[F(1,\bar{x}_p) - F(1,0)] + 0.5F(0,\bar{x}_p) - \bar{x}_p F(1,0)}{\alpha_N + \bar{x}_p + \bar{e}_p} - \frac{k_{nr}\overline{\omega}_g}{\alpha_N + \bar{x}_p + \bar{e}_p}$$

440 The $\overline{H}$ is deduced from the following relationship obtained for the depth, x_p (z = 0):

441 $$w_P^{IV} + \alpha_N w_P''' + 2\lambda^2 w_P'' = 0$$

442 where w_p'', w_p''', and w_p^{IV} are values of 2nd, 3rd, and 4th derivatives of $w(x)$ with respect to depth z. Given

443 $\bar{x}_p = 0$, the minimum head load to initiate slip is obtained.

444 (b) Normalised ground-line deflection, $\overline{w}_g$

445 $$\overline{w}_g = 4[F(4,\bar{x}_p) - F(4,0) - \bar{x}_p F(3,\bar{x}_p)] - 2(2\alpha_N^2 - 1)[F(2,\bar{x}_p) - F(2,0) - k_{nr}\overline{\omega}_g] - (2k_{nr}\bar{x}_p + 1)\bar{x}_p\overline{\omega}_g$$
$$- 2\alpha_N F(1,\bar{x}_p) - 2F(2,0)\bar{x}_p^2 + 2[F(1,0) + \overline{H}][\frac{-1}{3}\bar{x}_p^3 + (2\alpha_N^2 - 1)\bar{x}_p + \alpha_N)] + 2\bar{e}_p\overline{H}[2\alpha_N^2 - 1 - \bar{x}_p^2]$$

446 The w_g is deduced from $w(x)$.

447 (c) Normalised rotation at ground level, $\overline{\omega}_g$

448 $$\overline{\omega}_g = \frac{4(\bar{x}_p + \alpha_N + \bar{e}_p)[F(3,\bar{x}_p) - F(3,0)] - 2(\bar{x}_p^2 - 2\alpha_N^2 + 1 + 2\bar{x}_p\bar{e}_p)F(2,\bar{x}_p)}{2k_{nr}(\bar{x}_p^2 + 2\alpha_N\bar{x}_p + 2\alpha_N^2 - 1) + \bar{x}_p + \alpha_N + \bar{e}_p}$$
$$- \frac{2(\bar{x}_p^2 + 2\alpha_N\bar{x}_p + 2\alpha_N^2 - 1)F(2,0) + 2[\bar{x}_p(\alpha_N\bar{x}_p + 2\alpha_N^2 - 1) + \bar{e}_p(2\alpha_N\bar{x}_p + 2\alpha_N^2 - 1)]F(1,\bar{x}_p)}{2k_{nr}(\bar{x}_p^2 + 3\alpha_N\bar{x}_p + 2\alpha_N^2 - 1) + \bar{x}_p + \alpha_N + \bar{e}_p}$$
$$- \frac{[\bar{x}_p^2 + 2\alpha_N\bar{x}_p + 1 + 2(\alpha_N + \bar{x}_p)]F(0,\bar{x}_p) - 2\bar{e}_p(\bar{x}_p^2 + 2\alpha_N\bar{x}_p + 2\alpha_N^2 - 1)F(1,0)}{2k_{nr}(\bar{x}_p^2 + 3\alpha_N\bar{x}_p + 2\alpha_N^2 - 1) + \bar{x}_p + \alpha_N + \bar{e}_p}$$

449 (d) Normalised ground-level bending moment

450 $$-\overline{M}_o = \overline{H}\bar{e}_p + k_{nr}\overline{\omega}_g$$

451 Finally it should be mentioned that the constants C_j are determined using the compatibility
452 conditions of $Q(\bar{x})$, $M(\bar{x})$, $w'(\bar{x})$, and $w(\bar{x})$ at the normalised slip depth, $\bar{x}_p$ [$\bar{x} = \bar{x}_p$ or $\bar{z} = 0$].
453 Elastic solutions validated for $N_g < 2(kE_pI_p)^{0.5}$ is ensured by $L > L_c$ + max. x_p
454

455

456 Table 1 Key response and parameters for a pile in 10-pile group

w_g (mm)	$\bar{x}_p$	$\overline{H}/\overline{w}_g$	H (kN)	$-\omega_g$ ($\times 10^{-3}$)	$C_5/-C_6$ ($\times 10^{-3}$)	$-M_o/-M_o^{FixH\ a}$ (kNm)	M_o/M_o^{FixH}
9.4	0.863	0.686/1.997	7.981	3.3035	4.154/1.574	5.43/12.29	0.442
23.5	1.34836	1.132/4.992	13.179	6.938	6.069/4.259	11.40/28.81	0.396
47.3	1.78227	*1.559/10.05*	18.616	12.0	7.964/7.462	19.43/51.5	0.377
83.1	2.17641	2.082/17.65	24.23	17.9	9.118/10.975	29.40/79.10	0.371

457 [a] Values of M_o^{FixH} is cited from Guo (2009).

458

Figure Captions

Fig. 1. Schematic model for a laterally loaded capped pile: (a) A single pile, (b) schematic model, (c) limiting force profile (LFP), (d) Pile deflection and w_p profiles, and (e) *p*-*y* curves for a single pile or a pile in a group.

Fig. 2. Nonlinear response of capped piles (n = 0.7): (a) load; (b) bending moment

Fig. 3. Nonlinear response of capped piles (n = 1.7): (a) load; (b) bending moment

Fig. 4. Nonlinear rotational slope of capped piles: (a) n = 0.7; (b) n = 1.7

Fig. 5. Non-dimensional profiles (n = 0.7): (a) displacement; (b) slope; (c) bending moment; and (d) shear force

Fig. 6. Non-dimensional profiles (n = 1.7): (a) displacement; (b) slope; (c) bending moment; and (d) shear force

Fig. 7. Predicted versus measured (Matlock et al. 1980) response of a pile in 10- pile group: (a) pile group layout; (b) p_u profile; (c) $w_g \sim H_{av}$ curves; (d) $-M_o \sim w_g$ curves; (e) moment profiles

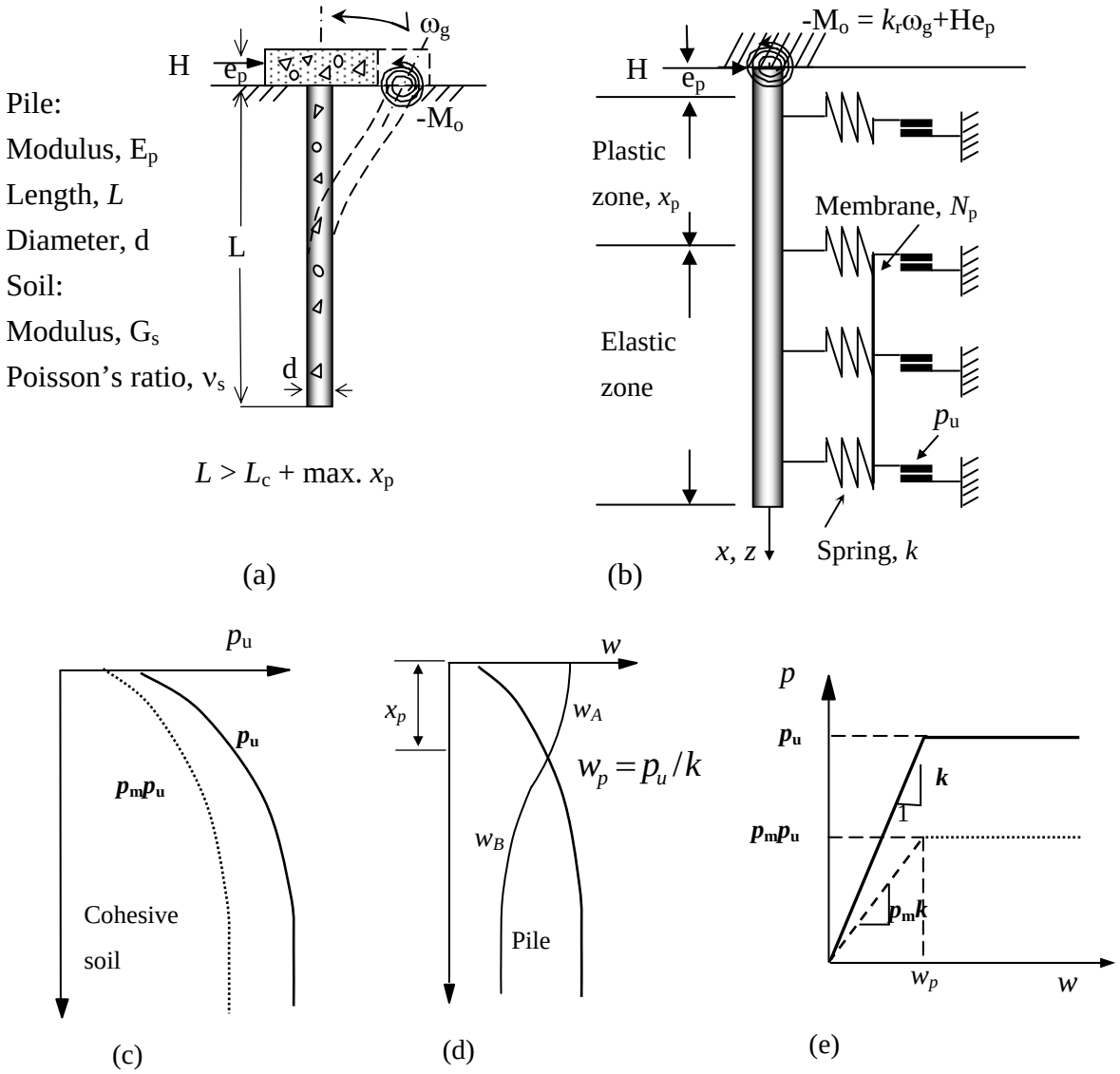

Fig.1. Schematic model for a laterally loaded capped pile: (a) a single pile; (b) schematic model; (c) limiting force profile (LFP); (d) Pile deflection and w_p profiles; and (e) p-y curves for a single pile or a pile in a group.

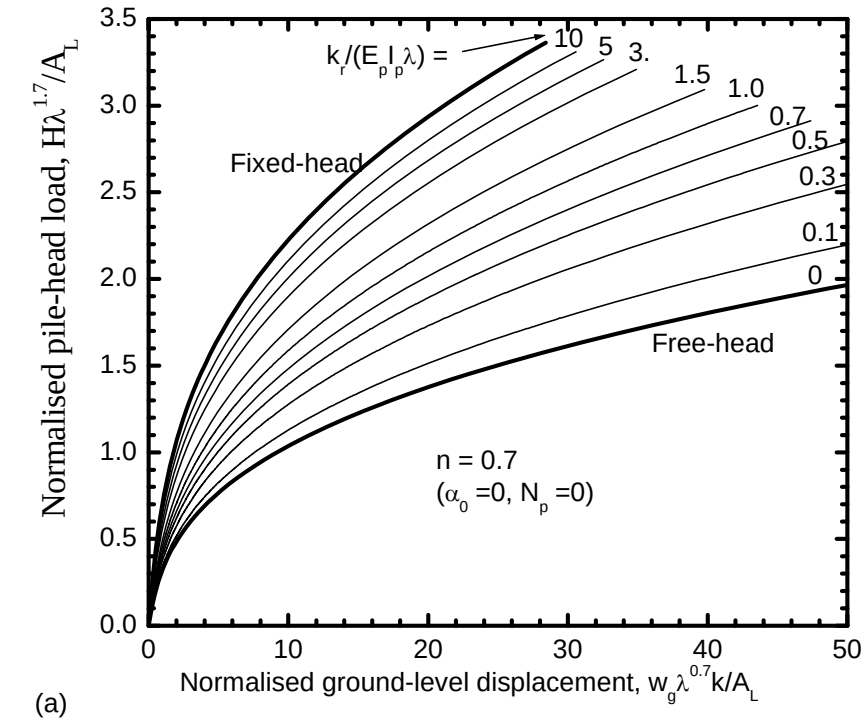

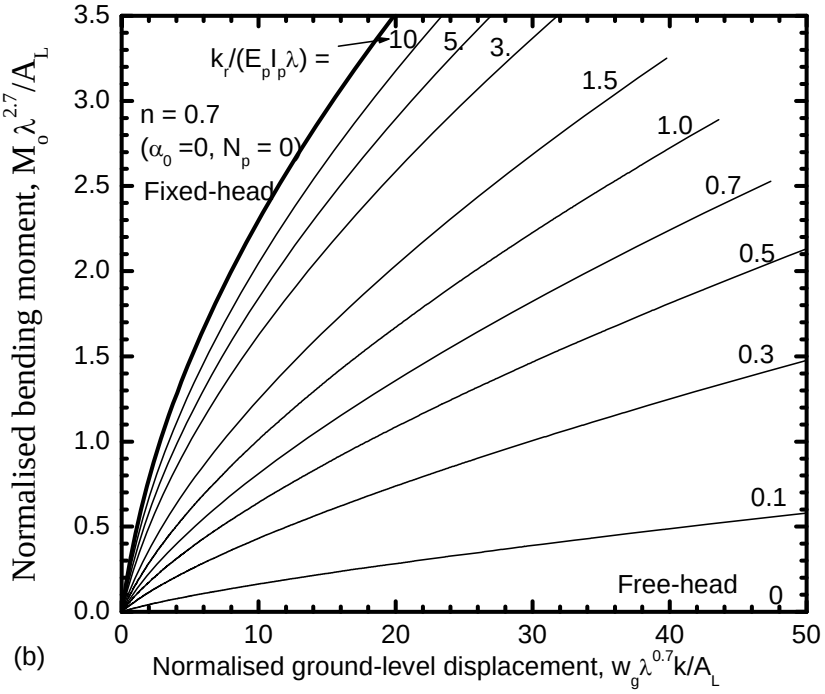

Fig. 2. Nonlinear response of capped piles (n = 0.7): (a) load; (b) bending moment

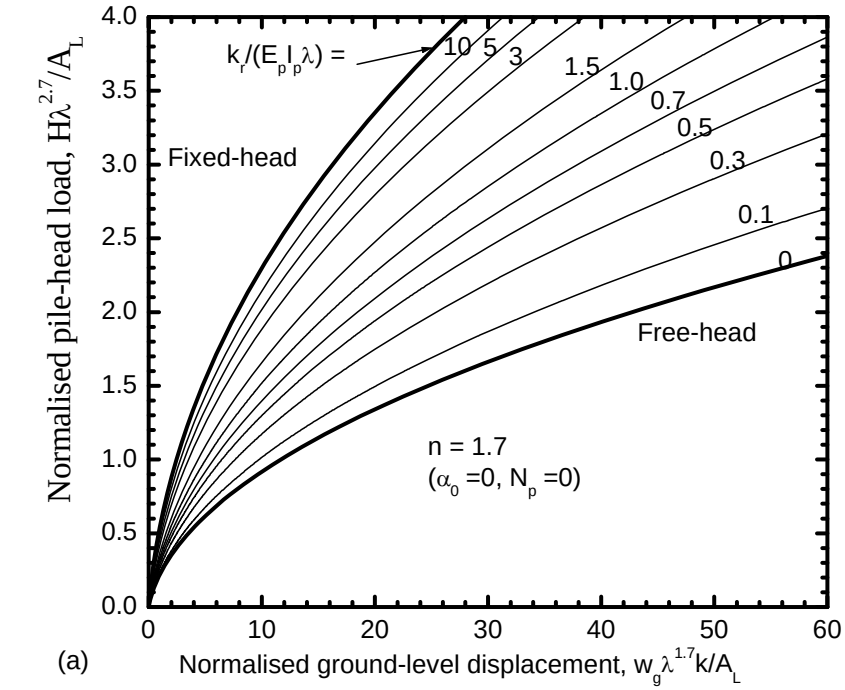

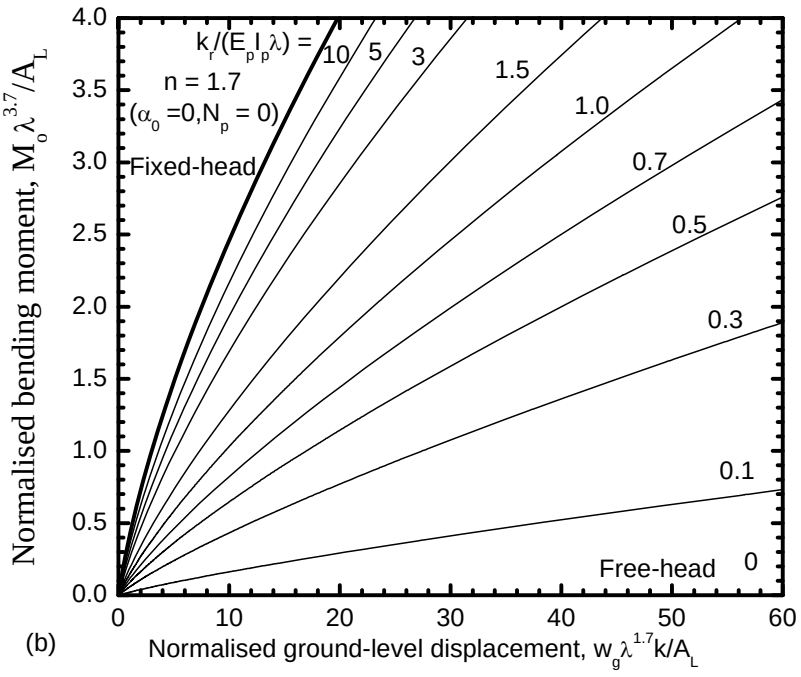

Fig. 3. Nonlinear response of capped piles (n = 1.7): (a) load; (b) bending moment

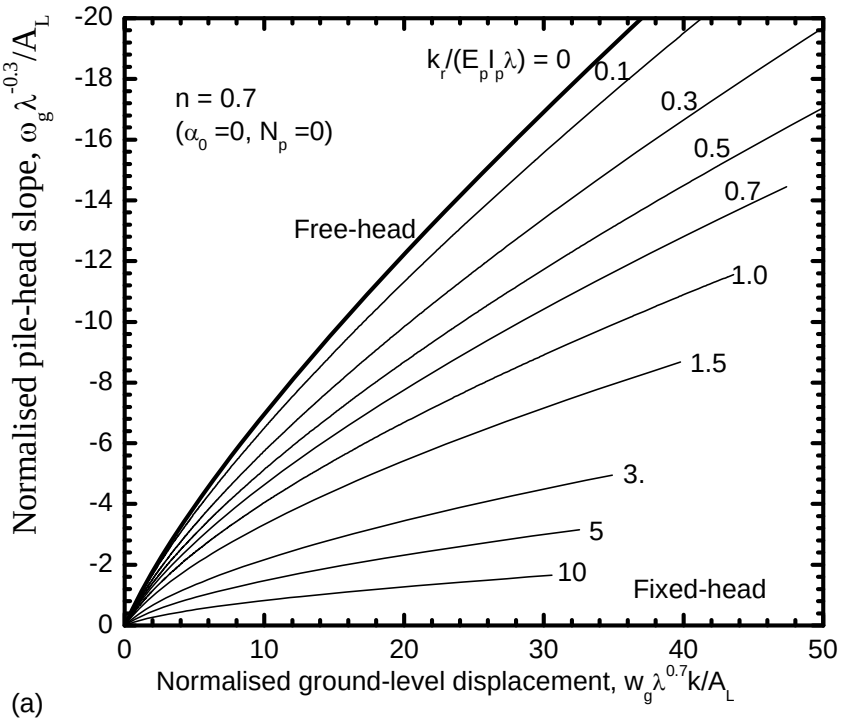

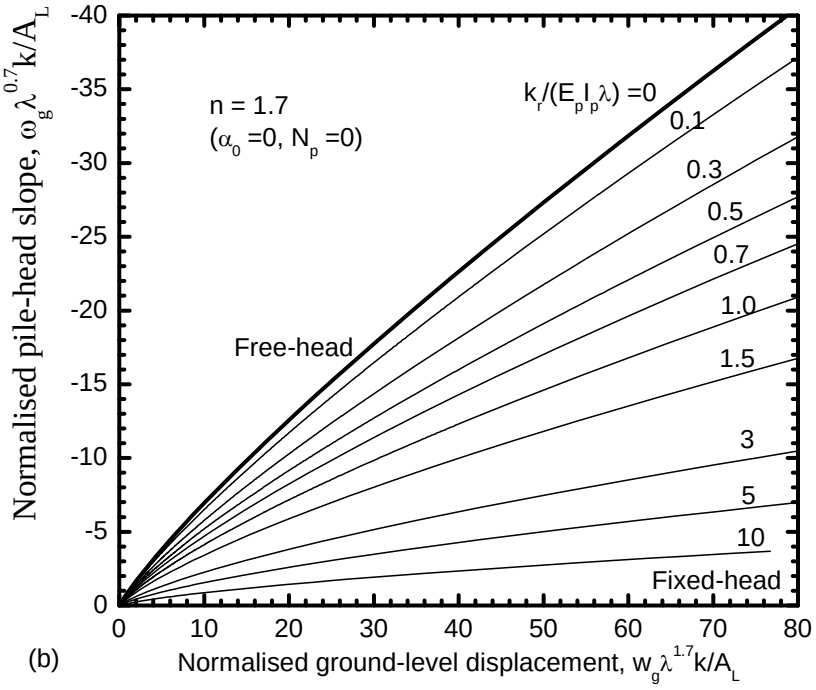

Fig. 4. Nonlinear rotational slope of capped piles: (a) n = 0.7; (b) n = 1.7

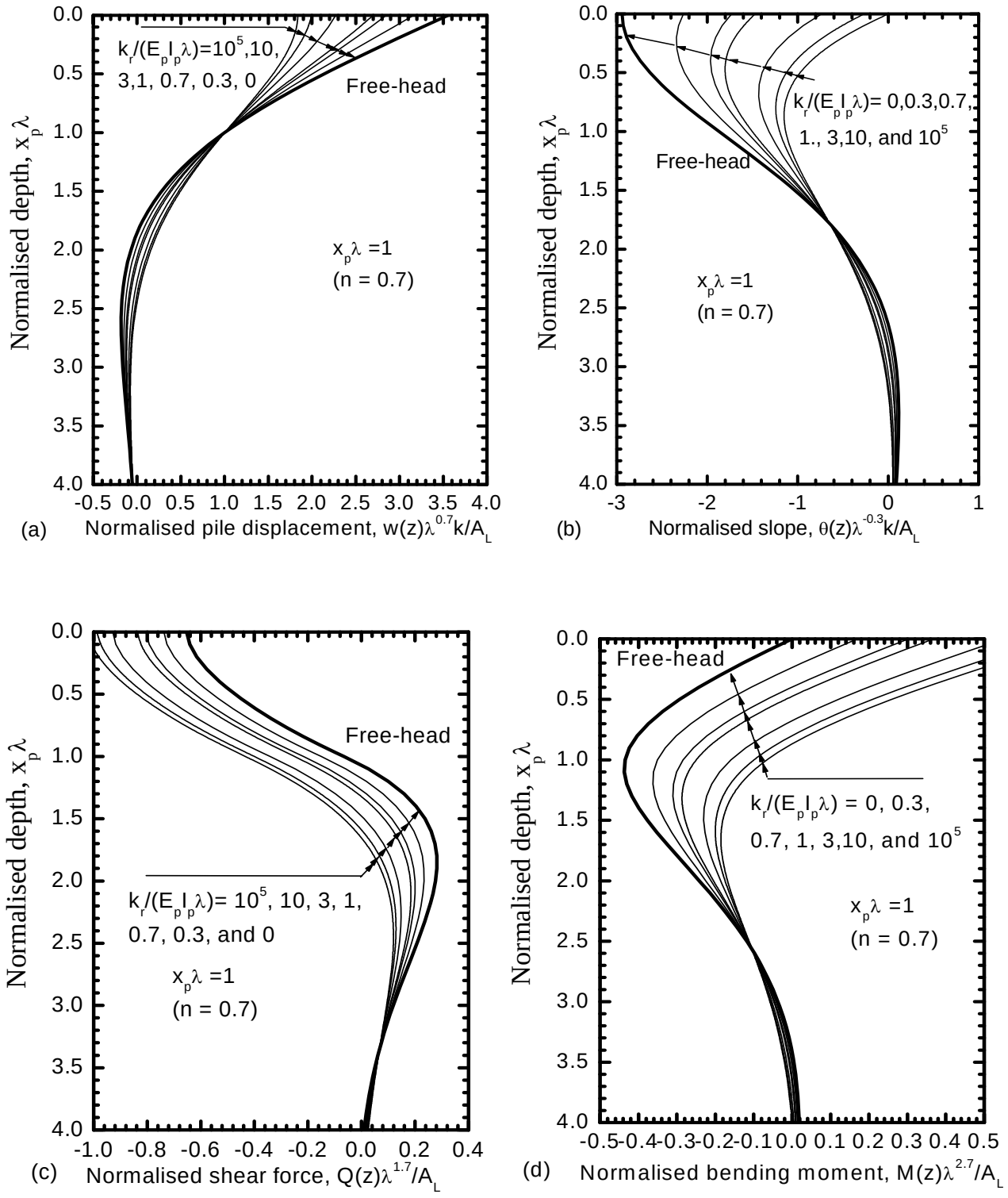

Fig. 5. Non-dimensional profiles (n = 0.7): (a) displacement; (b) slope; (c) bending moment; and (d) shear force

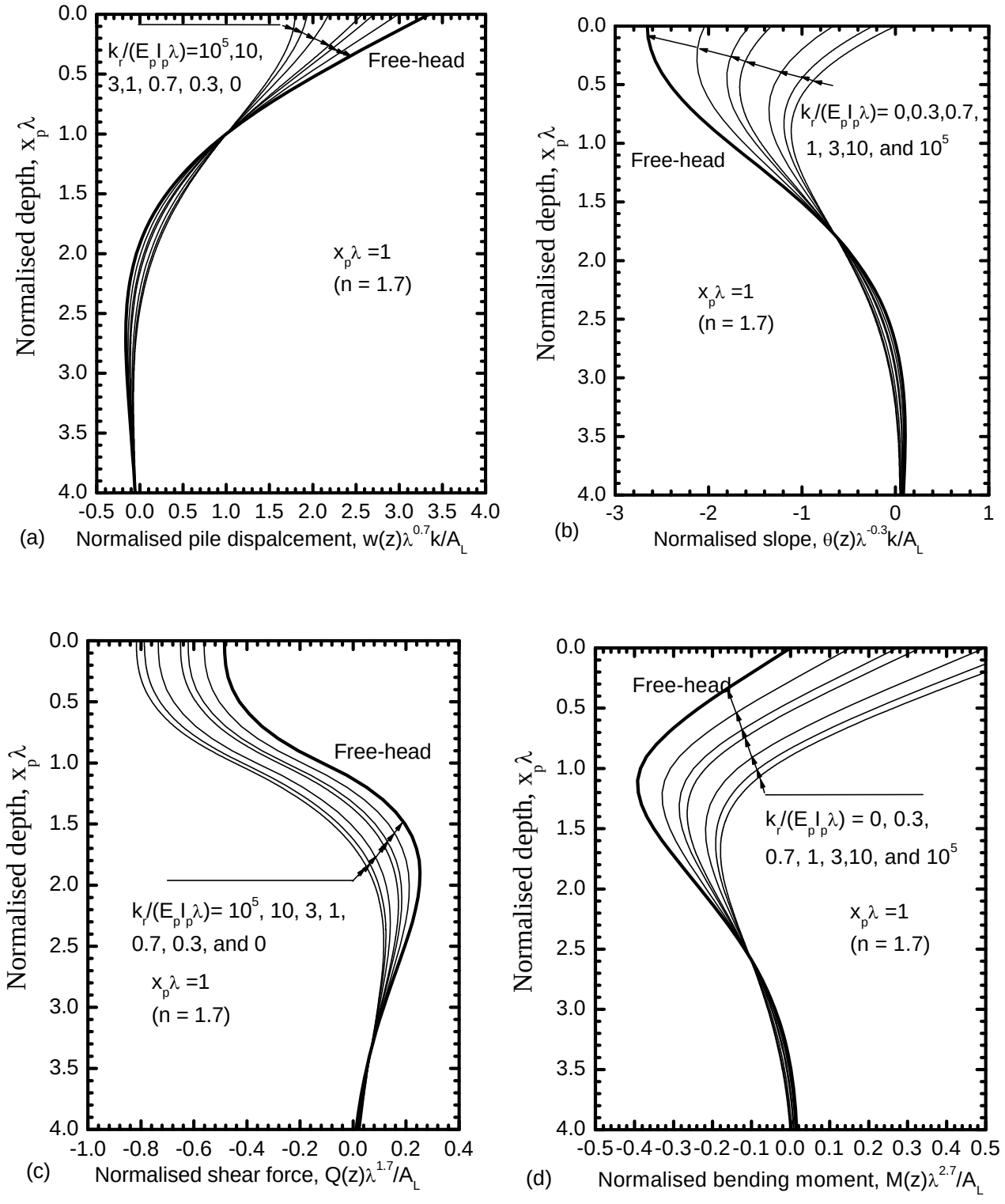

Fig. 6. Non-dimensional profiles (n = 1.7): (a) displacement; (b) slope; (c) bending moment; and (d) shear force

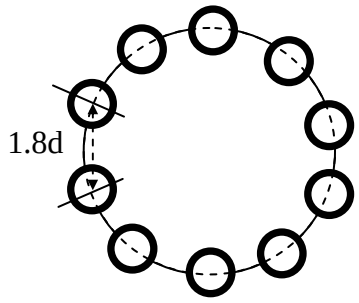

(a) Layout of the 10-pile groups

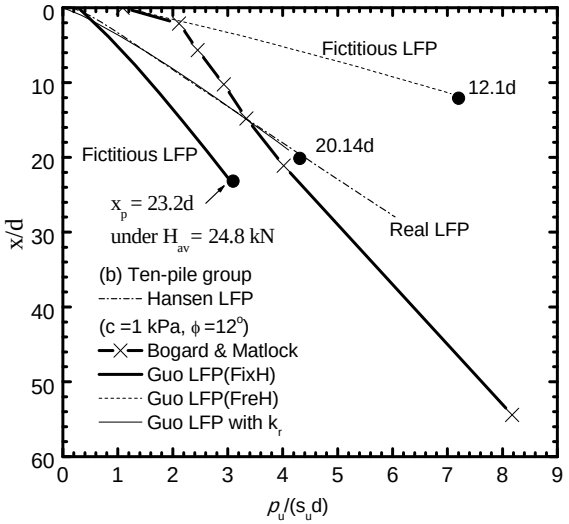

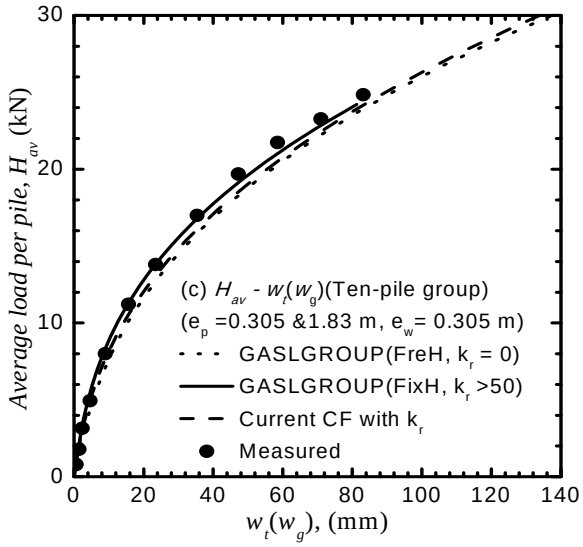

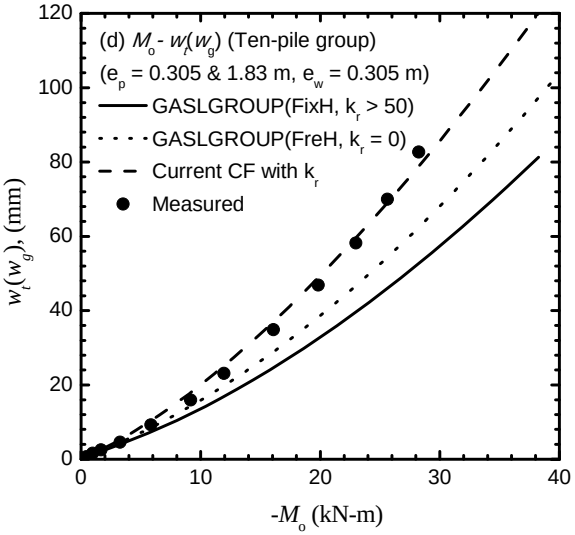

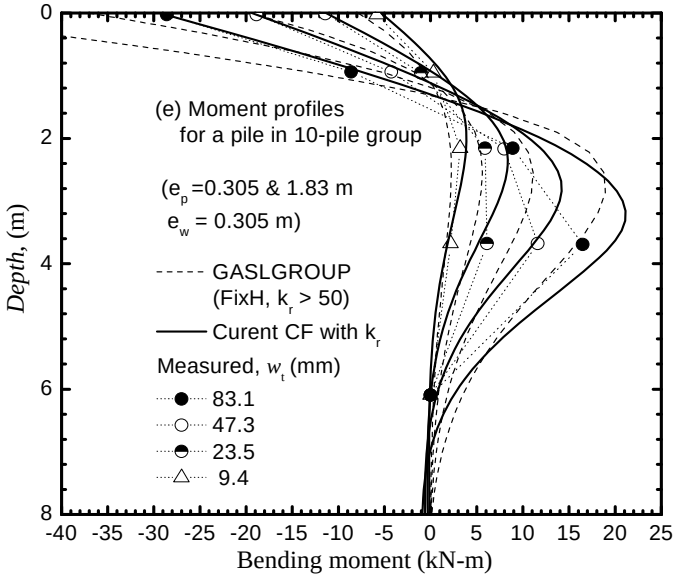

Fig.7. Predicted versus measured (Matlock et al. 1980) response of a pile in 10- pile group: (a) pile group layout; (b) p_u profile; (c) w_g ~ H_{av} curves; (d) $-M_o$~w_g curves; (e) moment profiles